EARTHQUAKE ENGINEERING AND STRUCTURAL DYNAMICS, VOL. 26, 1005–1019 (1997)

EFFECTS OF THE DYNAMIC CROSS-INTERACTION IN THE SEISMIC ANALYSIS OF MULTIPLE EMBEDDED FOUNDATIONS

R. BETTI*†

Department of Civil Engineering and Engineering Mechanics, Columbia University, New York, NY 10027, U.S.A.

SUMMARY

A boundary element formulation of the substructure deletion method is presented for the seismic analysis of the dynamic cross-interaction between multiple embedded foundations. This approach is particularly suitable for three-dimensional foundations of any arbitrary geometrical shape and spatial location, since it requires only the discretization of the foundations' surfaces. The surrounding soil is represented by a homogeneous viscoelastic half-space while the foundations are assumed to be rigid and subjected to incoming SH-, P-, and SV-waves arbitrarily inclined in both the horizontal and vertical planes. The proposed methodology is tested for the case of two identical embedded square foundations for different values of the foundations' embedment and distance. The effects of the cross-interaction are outlined in the components of the impedance matrix and of the foundation input motion. © 1997 John Wiley & Sons, Ltd.

Earthquake Engng. Struct. Dyn., **26**, 1005–1019 (1997)

No. of Figures: 9. No. of Tables: 0. No. of References: 15.

KEY WORDS: Soil–structure interaction; embedded foundations; boundary element method; seismic analysis of foundations; cross-interaction

INTRODUCTION

In the analysis and design of structures subjected to earthquake excitation, the dynamic interaction between the foundations and the surrounding soil plays a fundamental role. When dealing with closely spaced structures or with structures on relatively close supports, the cross-interaction through the soil between adjacent foundations might also be important for the solution of some practical problems. Although soil–structure interaction problems have been extensively investigated over the last thirty years, relatively little attention has been given to problems associated with the cross-interaction through the soil between adjacent embedded foundations.

As in the case of an isolated foundation, the crucial task in the analysis of multiple foundations subjected to earthquake excitation is represented by the determination of the force–displacement relationship (impedance matrix) for the excavated half-space. In fact, in linear dynamic soil–structure interaction, the seismic response of a foundation system can be decomposed into the response due to external and inertial forces, and the foundation input motion. Both contributions can be easily obtained after the impedance matrix for the foundation system and the free-field ground motion are computed. The free-field ground motion, which corresponds to the soil response prior to any excavation, can be determined using classical wave propagation theory whereas the determination of the force–displacement relationship requires the solution of a very complicated mixed boundary value problem in elastodynamics. The computation of the frequency-dependent impedance matrix for the foundations system represents the most challenging problem in dynamic soil–structure interaction.

* Correspondence to: R. Betti, Department of Civil Engineering and Engineering Mechanics, Columbia University, 610 Seeley W. Mudd Building, New York, NY 10027-6699, U.S.A.
† Associate Professor

CCC 0098–8847/97/101005–15$17·50
© 1997 John Wiley & Sons, Ltd.
Received 17 October 1996
Revised 11 March 1997

Due to the complexity of the problem, most of the present studies on the cross-interaction between adjacent foundations neglect the effect of the embedment of the foundation into the soil and restrict their analyses to surface foundations.[1,2] Triantafyllidis and Neidhart[3] analysed the dynamic cross-interaction between two rigid circular surface foundations subjected to Rayleigh waves impinging at an arbitrary angle, showing that, in addition to loads along the direction of incidence of the incoming wave, additional loads perpendicular to the direction of progation act on the foundations due to scattered waves. The effects of the foundation mats' flexibility on the cross-interaction between surface foundations were included by Wang *et al.*[4] and Qian *et al.*[5] while the coupling between the superstructure and a multiple surface foundations system was investigated by Werner *et al.*[6], who analyzed the three-dimensional response of a soil–bridge system subjected to incoming plane SH-waves.

In most practical engineering applications, depending upon the soil conditions and the structural type, the foundations are partially or totally embedded in the ground and the effects of the surrouding soil greatly alter their static and dynamic response. As with the single foundation case, when the effect of the embedment is included in the multiple foundations case, analytical difficulties and enormous numerical calculations have limited the analysis to two-dimensional problems or to three-dimensional analyses of foundations of relatively simple geometry. Luco and Contesse[7] studied the two-dimensional, antiplane, building–soil–building interaction for two shear walls placed on rigid circular foundations and subjected to vertically incident plane SH-waves while Abdel-Ghaffar and Trifunac[8] analysed a simplified 2-D bridge model with hemispherical foundations subjected to inclined SH-waves.

The importance of the embedment in the through-the-soil interaction was also pointed out by Lysmer *et al.*[9] in a two-dimensional analysis of the cross-interaction between a nuclear containment building and two adjacent buildings subjected to ground motion. The results showed that the peak response of the containment building was amplified by a factor of two and a half with respect to that obtained without the two adjacent structures. A parametric study on the relative significance of various factors affecting the dynamic interaction between adjacent embedded foundations was presented by Lin *et al.*[10] They used a hybrid approach which considers a finite element representation for the near field while, in the far field, waves are expressed in terms of semidiscrete modes of vibration and particular solutions. The results confirmed that the motions induced in the neighbouring foundation are comparable with those of the excited foundation and that these effects depend on the embedment and distance between the foundations.

The dynamic structure–soil–structure interaction between adjacent three-dimensional structures was investigated by Wang and Schmid[11], who studied two identical structures on embedded foundations subjected to a harmonic concentrated force applied at one of the nodal points. Their results confirmed that the distance between the two structures greatly influences the through-the-soil interaction and its effects are more noticeable as the distance decreases.

The investigation undertaken herein presents an efficient methodology for the through-the-soil interaction analysis of three-dimensional embedded foundations of arbitrary shape, subjected to seismic waves impinging at an arbitrary angle. The proposed technique represents a boundary element formulation of the Substructure Deletion Method (SDM),[12] which has been successfully applied in the analysis of a single embedded foundation in both the 2-D[13] and 3-D[14] domains. Being the most challenging tasks in soil–structure interaction, this paper focuses on the determination of the frequency-dependent impedance matrix and of the foundation input motion for a system of three-dimensional embedded foundations of arbitrary shape.

DETERMINATION OF THE IMPEDANCE MATRIX FOR MULTIPLE EMBEDDED FOUNDATIONS

In the seismic analysis of embedded foundation systems, the most difficult and challenging task is represented by the determination of the foundations' impedance matrix. It requires the solution of a radiation boundary-value problem for an excavated half-space, as shown in Figure 1. If N_f denotes the total number of

 © 1997 John Wiley & Sons, Ltd.

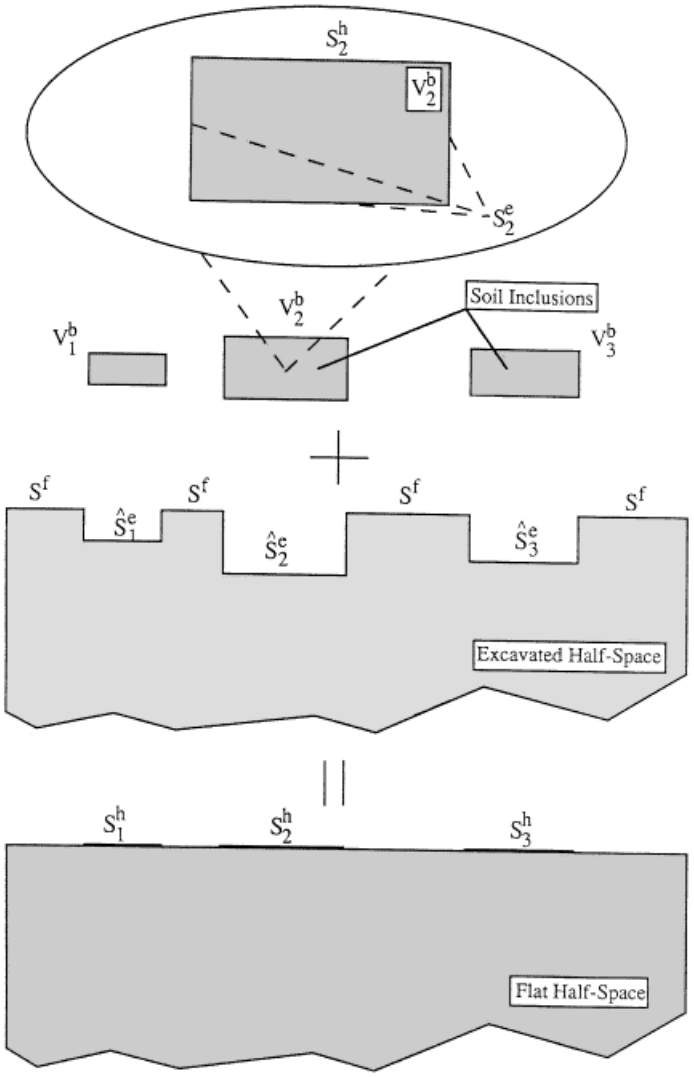

Figure 1. Excavated half-space and substructure deletion method for multiple foundations

embedded foundations, the boundary conditions of such a problem involve: (1) the condition of free-traction on the horizontal free surface S^f, (2) the radiation condition at infinity, and (3) displacement and/or traction conditions along each embedded surface $\hat{S}_i^e$ ($i = 1, 2, \ldots, N_f$).

For an efficient solution of such a problem, valid for both 2-D and 3-D embedded foundations of arbitrary shape, an approach based on the Substructure Deletion Method[14] is proposed. For the multiple embedded foundations case, the basic assumption of the SDM states that if the volumes V_i^b ($i = 1, 2, \ldots, N_f$) of the same material of the excavated half-space are inserted into the cavities occupied by the foundations and welded contact is assumed along the embedded boundaries $\hat{S}_i^e$ ($i = 1, 2, \ldots, N_f$), the flat viscoelastic half-space is recreated (Figure 1). Hence, the solution of the radiation problem in the case of multiple embedded foundations can be obtained from the separate analysis of the unexcavated half-space (exterior problem) and from the analysis of the N_f bounded domains V_i^b (interior problems). These finite domains represent the

© 1997 John Wiley & Sons, Ltd.

portions of soil removed during the excavation and replaced by the foundations. In this study, a formulation based on the Boundary Element Method (BEM) has been used in the analysis of the exterior problem and of the various interior problems. This formulation has already been successfully applied for the analysis of a single embedded foundation.[14] The main advantages of this approach are: (1) the BEM is used in the analysis of both types of problems (exterior and interiors), avoiding problems associated with the compatibility and accuracy of different methods, (2) compared with a classical BEM formulation, it does not require the discretization of the flat surface between the foundations and the truncation of the distant free surface, and (3) it can be applied to foundations of arbitrary geometrical shape and with any spatial location.

FORMULATION OF THE SUBSTRUCTURE DELETION METHOD

Following the methodology presented in Reference 14, consider the finite domain V_i^{b} $(i = 1, 2, \ldots, N_f)$ of the same material of the excavated half-space, bounded by external surface S_i $(S_i = S_i^e \cup S_i^h)$, as shown in Figure 1. Using a Direct Boundary Element (DBEM) discretization with constant elements and full-space Green's functions for the displacements and tractions as fundamental solutions, it is possible to write a force–displacement relationship for the ith inclusion as

$$\begin{Bmatrix} \mathbf{u}_h^i \\ \mathbf{u}_e^i \end{Bmatrix} = \begin{bmatrix} C_{hh}^i & C_{he}^i \\ C_{eh}^i & C_{ee}^i \end{bmatrix} \begin{Bmatrix} \mathbf{t}_h^i \\ \mathbf{t}_e^i \end{Bmatrix} \tag{1}$$

where $\{\mathbf{u}_h^i\}$ and $\{\mathbf{t}_h^i\}$ indicate the displacement and traction components for the elements on S_i^h and $\{\mathbf{u}_e^i\}$ and $\{\mathbf{t}_e^i\}$ the corresponding components for the elements on S_i^{e}. The partitioned matrix $[C^i]$ represents the compliance matrix of the ith finite inclusion; its elements depend on the frequency, on the geometry of S_i and on the soil properties.

When the finite inclusion of soil are inserted into the various cavities and the equilibrium and compatibility conditions for the displacements are imposed over each embedded surface S_i^{e} $(i = 1, 2, \ldots, N_f)$, the flat viscoelastic half-space is recreated (Figure 1). Considering the same boundary element discretization for each S_i^h (N_{hi} elements on S_i^h, $i = 1, 2, \ldots, N_f$), as used in the corresponding interior problem, and using half-space Green's functions as fundamental solutions lead to a force–displacement relation for the set of flat surfaces S_i^h $(i = 1, 2, \ldots, N_f)$ as

$$\{\mathbf{u}_h^f\} = [C_{hh}^f]\,\{\mathbf{t}_h^f\} \tag{2}$$

where the superscript f indicates quantities related to the flat half-space. The matrix $[C_{hh}^f]$, of dimension $3(N_f \times N_{hi}) \times 3(N_f \times N_{hi})$, is a full matrix and represents the 'compliance matrix' for the flat surface $S_t^h = S_1^h \cup S_2^h \cup \cdots \cup S_{N_f}^h$.

It is evident from equations (2) that the exterior problem can be considered as an interaction problem between the horizontal surfaces S_i^h. This requires only the discretization of the surfaces S_i^h, avoiding the problems associated with the discretization of the free surface between the foundation blocks and with the truncation of the distant free surface. Only the discretization of the flat surfaces S_i^h $(i = 1, 2, \ldots, N_f)$ and of the embedded surfaces S_i^e $(i = 1, 2, \ldots, N_f)$ is required.

After the exterior and the N_f interior problems have been analysed (equations (1) and (2)), the compliance matrix $[\hat{C}]$ for the embedded surface $\hat{S}_t^e = \hat{S}_1^e \cup \hat{S}_2^e \cup \cdots \cup \hat{S}_{N_f}^e$ can be easily obtained by using the Substructure Deletion formulation. If each of the bounded domains V_i^{b} $(i = 1, 2, \ldots, N_f)$ is placed into the corresponding cavity and the compatibility conditions for the displacements and the equilibrium conditions are satisfied over each $\hat{S}_i^e$ $(i = 1, 2, \ldots, N_f)$, then the flat half-space is restored.

By manipulating the solutions for the N_f interior problems (equations (1)) and exterior problem (equations (2)),[14] it is possible to obtain the required force–displacement relation for the excavated infinite half-space, as

$$\{\hat{\mathbf{u}}_e\} = [-[C_{eh}[[C_{hh}^f] - [C_{hh}]]^{-1}[C_{he}] - [C_{ee}]]\{\hat{\mathbf{t}}_e\} \tag{3}$$

 © 1997 John Wiley & Sons, Ltd.

where $\{\hat{\mathbf{u}}_e\}$ and $\{\hat{\mathbf{t}}_e\}$ represent the displacement and traction vectors, respectively, for points $\hat{S}_t^e$ in the excavated unbounded soil. The matrix

$$[\hat{C}] = -[C_{eh}][[C_{hh}^f] - [C_{hh}]]^{-1}[C_{he}] - [C_{ee}] \tag{4}$$

represents the compliance matrix for the embedded surface $\hat{S}_t^e$ in the unbounded excavated half-space. Such a matrix is dependent on: (1) the frequency of the excitation, (2) the geometry of each foundation and their relative location, and (3) the soil properties. The impedance matrix $[\hat{K}]$ for the multiple foundations system can be easily obtained by inverting the compliance matrix $[\hat{C}]$.

It is noteworthy that, even though the general expression of the compliance matrix for multiple embedded foundations (equations (4)) is formally identical to the one of a single embedded foundation,[14] the structure and the meaning of the various submatrices $[C_{hh}^f]$, $[C_{hh}]$, $[C_{he}]$, $[C_{eh}^f]$ and $[C_{ee}]$ are completely different. For the case of a single embedded foundation, these matrices are all full while, for the multiple foundations case, only $[C_{hh}^f]$ is full and the other matrices are block diagonal

$$[C_{lk}] = \begin{bmatrix} [C_{lk}^1] & [0] & \cdots & [0] \\ [0] & [C_{lk}^2] & \cdots & [0] \\ [0] & \vdots & \ddots & [0] \\ [0] & \cdots & [0] & [C_{lk}^{N_f}] \end{bmatrix}$$

For the case of two adjacent foundations, the compliance matrix $[\hat{C}]$ has the following expression:

$$[\hat{C}] = -\begin{bmatrix} [C_{eh}^1] & [0] \\ [0] & [C_{eh}^2] \end{bmatrix}\left[\begin{bmatrix} [C_{hh}^{f11}] & [C_{hh}^{f12}] \\ [C_{hh}^{f21}] & [C_{hh}^{f22}] \end{bmatrix} - \begin{bmatrix} [C_{hh}^1] & [0] \\ [0] & [C_{hh}^2] \end{bmatrix}\right]^{-1}$$
$$\begin{bmatrix} [C_{he}^1] & [0] \\ [0] & [C_{he}^2] \end{bmatrix} - \begin{bmatrix} [C_{ee}^1] & [0] \\ [0] & [C_{ee}^2] \end{bmatrix}$$

It is through the full matrix $[C_{hh}^f]$ and through the term $[[C_{hh}^f] - [C_{hh}]]^{-1}$ that the coupling due to the cross interaction through the soil is brought into the analysis

DETERMINATION OF THE FOUNDATION INPUT MOTION

Once the solution of the radiation problem has been obtained, it is then possible to easily determine the foundation input motion for the multiple foundations system. Such an input motion represents the response of massless foundations subjected to incoming seismic waves, the foundations' mass being included at a later stage. This response depends on the frequency, type and angle of incidence of the seismic waves, on the shape of the foundations and their relative location, and on the properties of the surrounding soil. Indicating with $\mathbf{U}_g(\mathbf{x})$ and $\mathbf{T}_g^n(\mathbf{x})$ the free-field displacement and traction vectors, respectively, at a point $\mathbf{x}$ located on the embedded surface $\hat{S}_t^e$ and introducing the assumption of rigid foundation blocks, the foundation input motion vector $\mathbf{U}_0^\star$ for the embedded rigid foundations can be expressed as

$$\mathbf{U}_0^\star = [C_0]\left(\int_{\hat{S}_t^e} [\Lambda]^{\mathrm{T}}[\hat{K}]\,\mathbf{U}_g(\mathbf{x})\,\mathrm{d}S(\mathbf{x}) + \int_{\hat{S}_t^e} [\Lambda]^{\mathrm{T}}\mathbf{T}_g^n(\mathbf{x})\,\mathrm{d}S(\mathbf{x})\right) \tag{5}$$

where $\mathbf{x} \in \hat{S}_t^e$, $[C_0]$ is the $6N_f \times 6N_f$ rigid body compliance matrix, $[\Lambda]$ is the rigid-body influence matrix for the foundation blocks and $[\hat{K}]$ is the impedance matrix for the embedded surface $\hat{S}_t^e$.

© 1997 John Wiley & Sons, Ltd.

Once the impedance matrix and the foundation input motion have been computed, the total response of the embedded foundation system can be easily obtained by solving the equations of motion of the foundation blocks subjected to forces applied by the superstructure and by the surrounding soil, including inertial effects.

NUMERICAL EXAMPLES

The foundation system considered in this study is shown in Figure 2. It consists of two massless rigid three-dimensional foundations, each of base dimensions $2a \times 2a$ and depth h, spaced at a distance l and embedded in a uniform viscoelastic half-space. The complex P- and S-wave velocities can be expressed as

$$v_\alpha = v_\alpha^*(1 + 2iq_\alpha)^{1/2} \simeq v_\alpha^*(1 + iq_\alpha), \qquad v_\beta = v_\alpha^*(1 + 2iq_\beta)^{1/2} \simeq v_\beta^*(1 + iq_\beta)$$

where v_α^* and v_β^* correspond, approximately, to the real parts of the P- and S-wave velocities and $i = \sqrt{-1}$. The coefficients q_α and q_β represent the damping ratios of the P- and S-wave, respectively, and their values are chosen to be 0·001 and 0·0005 so as to approximate the purely elastic medium. These values will also enable us to compare the results for two adjacent foundations with those obtained for a single foundation,[14] in order to highlight the cross-interaction effects. The ratio between the P-wave velocity and the S-wave velocity in this study is equal to 2 (Poisson's ratio $\nu = 0{\cdot}333$).

For this three-dimensional analysis, two values of the embedment ratio ($h/a = 0{\cdot}333$ and 0·5) have been selected. Higher values of the embedment ratio have not been considered because, with respect to other methods, the three-dimensional substructure deletion approach has shown some discrepancies related to limitation in mesh refinement for high values of h/a. For lower values of the embedment ratio, the effects of the embedment are minimal and can be neglected, essentially reducing the embedded foundations problem to the case of surface foundations. In the range of low embedded ratios, the proposed approach is quite effective and the results converge to those obtained in the case of surface foundations.[2] Consequently, two values of the dimensionless distance between the two foundations, defined as the ratio between the foundations distance and half of the foundation base dimension, have been used ($l/a = 4$ and 10), representing the conditions of 'closely spaced foundations' and 'distant foundations' for the considered values of h/a. In

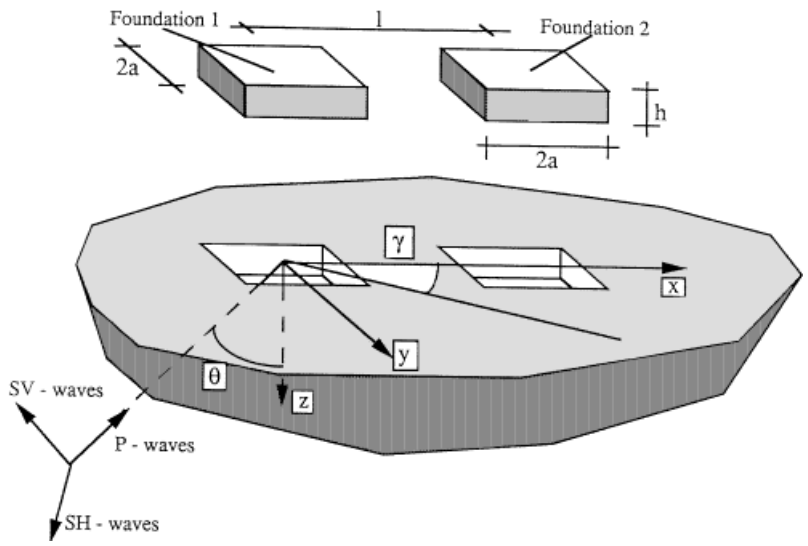

Figure 2. Case study: two embedded foundations subjected to incoming waves

 © 1997 John Wiley & Sons, Ltd.

presenting the results, when possible, preference will be given to the case of $h/a = 0.5$, since the cross-interaction effects are more relevant.

The assumption of rigid foundations implies that the motion of each foundation block can be described by the rigid-body displacement vector $\mathbf{U}_0^i$ ($i = 1, 2, \ldots, N_f$):

$$\mathbf{U}_0^i = \{\Delta_{0x}^i; \Delta_{0y}^i; \Delta_{0z}^i; a\Theta_{0x}^i; a\Theta_{0y}^i; a\Theta_{0z}^i\}^{\mathrm{T}}$$

with Δ_{0j}^i and Θ_{0j}^i representing the translational and rotational components of the displacement along the j-axis, with respect to a reference point, for the ith foundation. In each foundation block, the point located at a depth h on the vertical axis through the centre of the foundation base has been selected as the reference point. Consequently, the rigid-body assumption reduces the impedance matrix of the embedded foundations to a $6N_f \times 6N_f$ matrix, whose generic term can be expressed as

$$K_{ij} = \mu a(k_{ij} + \mathrm{i}a_0 c_{ij})$$

where μ is the Lame's constant and a_0 is the dimensionless frequency expressed as

$$a_0 = \frac{\omega a}{v_\beta^*}$$

For each of the 2 finite domains, an equally spaced mesh of 13×13 elements on the horizontal surfaces and of $13 \times 6 \times 4$ elements on the vertical surfaces has been used, based on the conclusions of.[14] The 'fictitious' eigenfrequencies associated with this boundary element discretization of the deleter are well above the frequency range of interest ($a_0 = 0.1$–2) and have no significant effect on the accuracy of the solution.[14]

The impedance matrix and the foundation input motion induced by arbitrarily inclined seismic waves for the two foundations system are analysed. The earthquake excitation is represented by plane SH-, P-, and SV-waves impinging at arbitrary angles in both the vertical and horizontal plane (Figure 2). The foundation input motion is presented in the form of its amplitude normalized with respect to the amplitude of the free field ground motion.

Impedance matrix

Figure 3 presents the magnitude of some elements of the dynamic impedance matrix of two adjacent foundations for the two values of the dimensionless distance and for an embedment ratio equal to 0.5. When possible, these elements are compared with those obtained from the analysis of a single foundation in order to outline the cross-interaction effects. Each element of the impedance matrix is identified by two indices which identify the element's location in the matrix. The displacements and rotations of the first foundation will be denoted by (1), (2), (3), and (4), (5), (6), respectively, while for the second foundation, they will be identified by (7), (8), (9) and (10), (11), (12). The translational impedances $K_{1,1}$ and $K_{2,2}$ (Figure 3) clearly show the effects of the cross interaction through the soil in the low frequency range. For two 'closely spaced' foundations ($l/a = 4$), the real part of the impedance function presents a slight increase (up to 12 per cent) with respect to the case of a single foundation. As expected, this increment is more evident in the component along the axis connecting the two foundations (x-axis, Figure 2) than in the component perpendicular to it. For higher frequencies and for 'distant' foundations, the impedance functions $k_{1,1}$ and $k_{2,2}$ approach the ones corresponding to the single foundation case. Similarly, the presence of a second foundation alters the radiation damping mechanism, especially in the low-frequency range, because of the scattering induced by the adjacent foundation. This phenomenon explains the decrease in the values of $c_{1,1}$ and $c_{2,2}$, a decrease that disappears in the high-frequency range or in the case of distant foundations (Figure 3). Also for these coefficients, the cross-interaction effects along the x-axis are more pronounced than those along a perpendicular direction (y-axis). The contributions to the horizontal forces from the rotations about the horizontal axes x and y seem to be slightly affected by the cross-interaction effects, more emphatically along the

© 1997 John Wiley & Sons, Ltd.

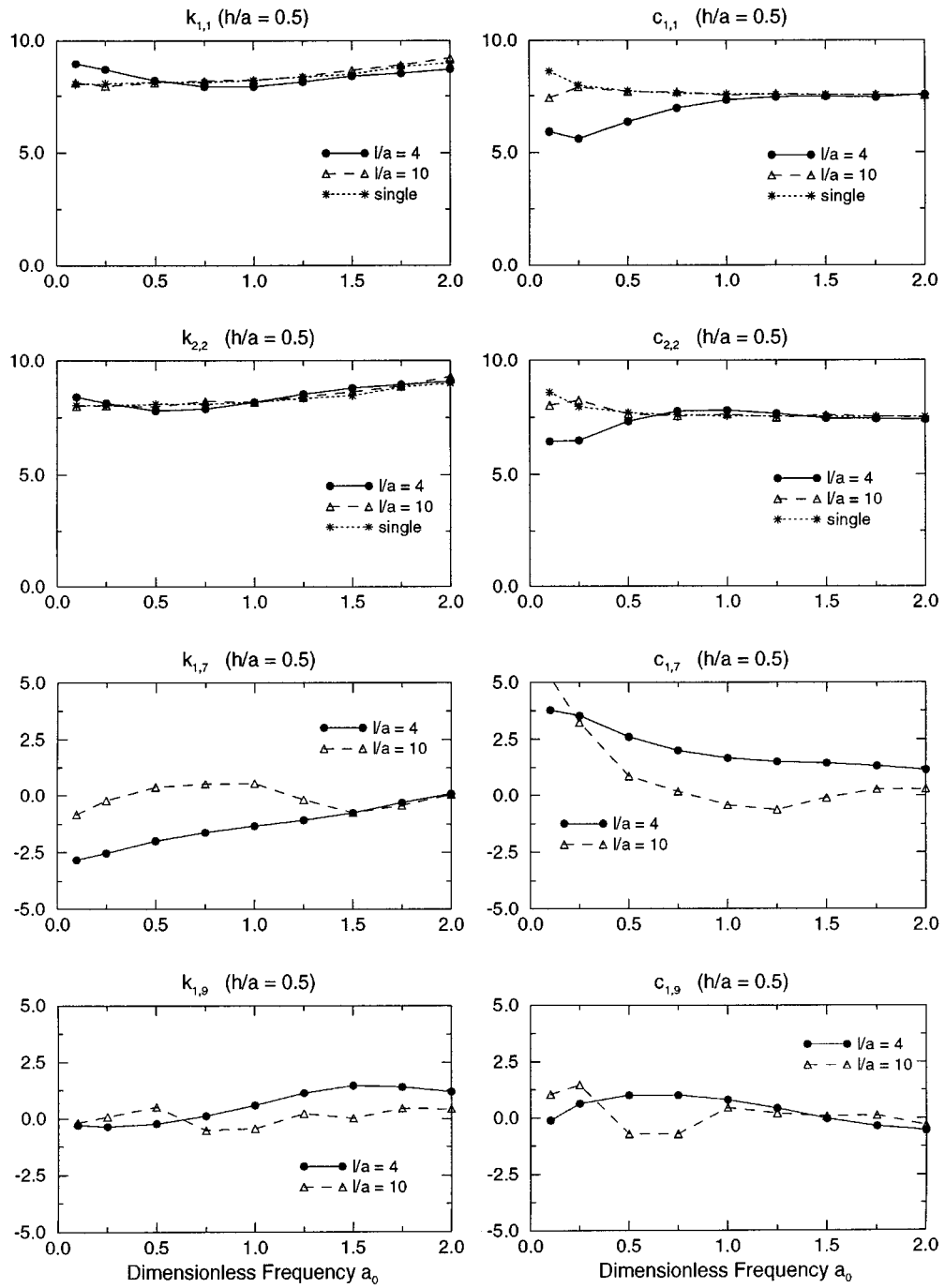

Figure 3. Horizontal translational impedances for foundation 1

direction of the axis connecting the two foundations. A similar conclusion was presented in Reference 10. The reduction of the imaginary component at low frequencies is still related to the decrease of radiation damping due to the presence of the adjacent foundation.

 © 1997 John Wiley & Sons, Ltd.

The cross-interaction effects between the two foundations are clearly manifested by the appearance of cross terms that would not appear in the case of isolated foundations. For the first foundation, contributions to the horizontal impedance along the x-axis by the motion of second foundations ($K_{1,9}$, $K_{1,7}$ and $K_{1,11}$) need to be considered (Figure 3): in the low-frequency range, the values of the real and imaginary components of $K_{1,7}$ reach about 30 per cent of the corresponding values of the horizontal impedance $K_{1,1}$. This represents a substantial contribution to the foundation response that cannot be neglected. By increasing the distance between the two foundations, these contributions decrease and the case of an isolated foundation is approached.

With regard to the rocking components, those associated with the horizontal displacement and rotation ($K_{4,2}$ and $K_{4,4}$, $K_{5,1}$ and $K_{5,5}$) remain practically unchanged. Also for these components, the cross terms (i.e. $K_{4,6}$, $K_{4,8}$, $K_{4,10}$ and $K_{4,12}$) account for the foundation–soil–foundation interaction. In the low-frequency range, the amplitudes of such components are comparable with those related to the case of a single foundation.

Identical conclusions can be obtained for the value of $h/a = 0{\cdot}333$. As expected, the decreased depth of the foundations slightly reduces the effects of the cross interaction, especially for the rocking components.

Foundation input motion: incoming SH-waves

First, consider vertically propagating SH-waves polarized in a direction perpendicular to the axis connecting the centers of the two foundations ($\theta = 0^\circ$ and $\gamma = 0^\circ$ in Figure 2). For both embedment ratios considered in this study, the two foundations present identical horizontal displacements along the y-axis and rotations about the x-axis (Figure 4). With regard to the horizontal component of the foundation response, the real part is predominant at low frequencies implying that the translational response is essentially in phase with the free-field motion at the center of the foundations. In the high-frequency range, the translational response, with reduced amplitude, increasingly becomes out of phase with respect to the free-field. The

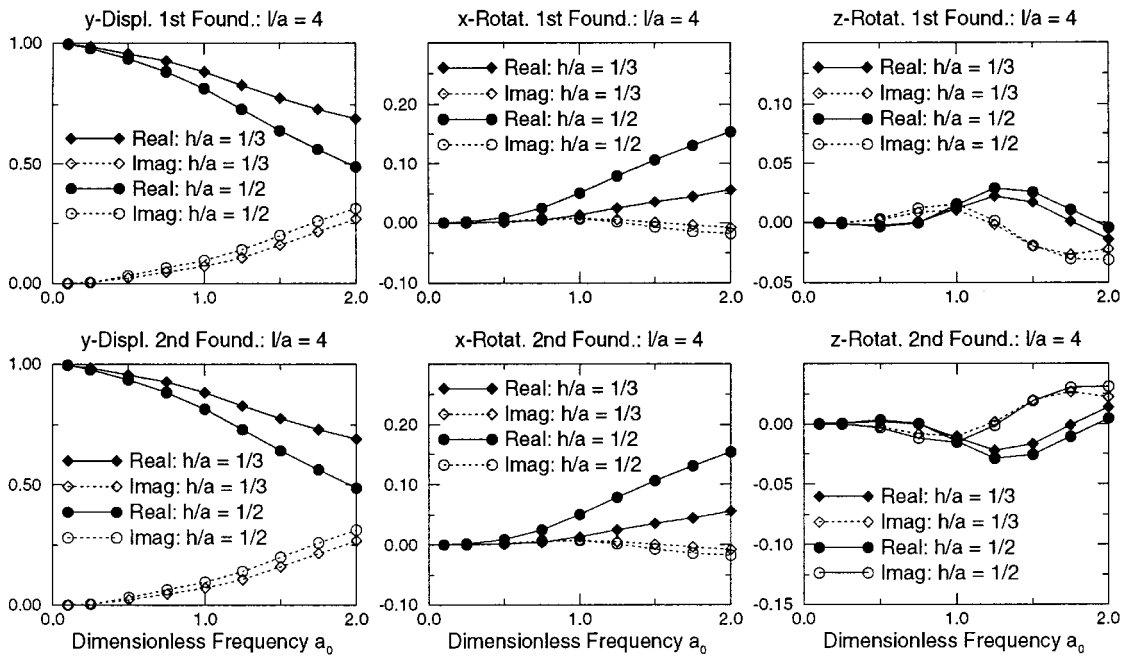

Figure 4. Foundation input motion: vertical SH-waves ($\theta = 0^\circ$, $\gamma = 0^\circ$, $1/a = 4$)

© 1997 John Wiley & Sons, Ltd.

displacement components associated with the rotations about the x-axis become more relevant at high frequencies, reaching up to 25 per cent of the translational components for $h/a = 0{\cdot}5$. It is important to point out that, with regard to the translational and rocking components, the two foundations move in phase with each other. The cross-interaction effects are evident in the displacement components associated with the rotation about the vertical axis. In fact, this torsional component of the foundation motion would not exist in the case of a single foundation subjected to vertically incident SH-waves. Such a result is confirmed by the amplitude reduction of the torsional component as the distance between the two foundations increases. These torsional components are of equal amplitude but opposite in phase (Figure 4).

For incoming SH-waves polarized along the y-axis but inclined of an angle θ ($\theta = 30^\circ$ ($h/a = 0{\cdot}5$; Figure 5) and 60°) the displacements along the y-axis and the rotations about the x-axis for foundation 1 show the same behavior as for the case of vertically incident SH-waves, with more drastic changes in amplitudes and marked differences in phase. Foundation 2 presents displacements in the y-direction whose amplitude, in the high frequency range, is 10 per cent lower than that of the first foundation. In addition, the two foundations move completely out of phase with respect to each other and to the free-field. In these two cases ($\theta = 30^\circ$ (Figure 5) and 60°), the rotations about the z-axis become predominant with respect to the rocking component. The amplitudes of such torsional components increase with frequency and differ for the two foundations. It is interesting to point out that, since the soil material is linear, the diagrams of the components of the foundation input motion for the second foundation for the case of $l/a = 4$ can be obtained by scaling the frequencies of the corresponding values obtained for $l/a = 10$ by a factor of 2.5.

For SH-waves arbitrarily inclined in both the vertical and horizontal planes, the foundation input motion of each foundation presents all six displacement components, whose amplitude and phase shift depend on the frequency of the incoming wave, and the two foundations move completely out-of-phase.

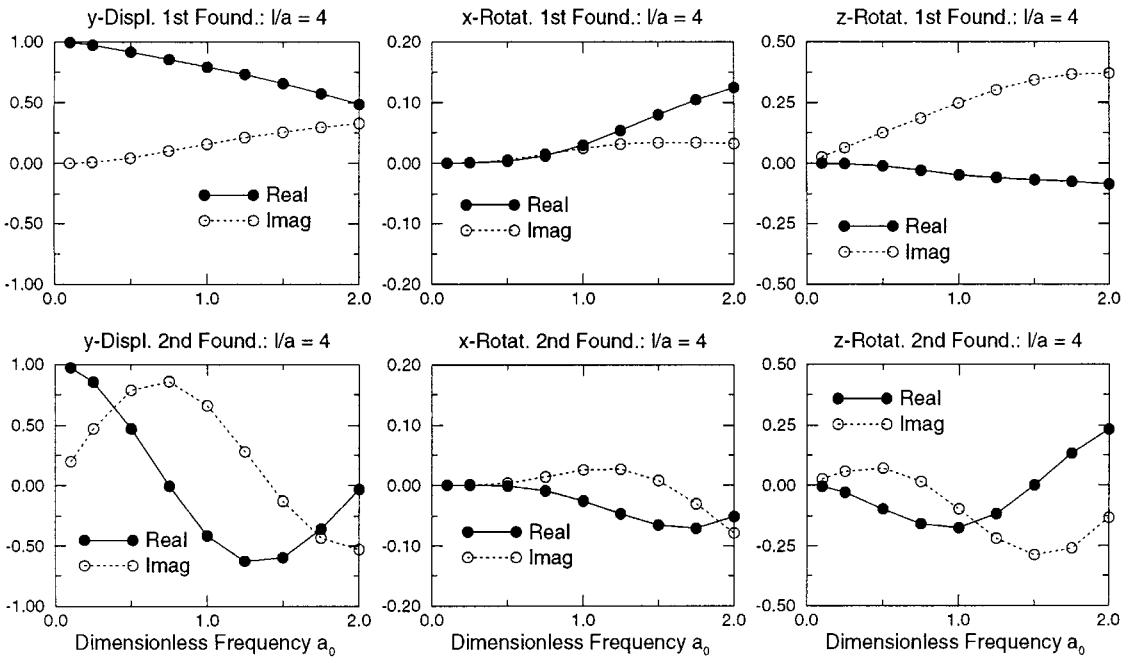

Figure 5. Foundation input motion: inclined SH-waves ($\theta = 30^\circ$, $\gamma = 0^\circ$, $1/a = 4$, $h/a = 0{\cdot}5$)

 © 1997 John Wiley & Sons, Ltd.

Foundation input motion: incoming P-waves

For vertically propagating P-waves, the two foundations present predominant displacement components along the vertical axis, which are of equal magnitude and in phase with each other. Similar to the case of vertically propagating SH-waves, when the frequency increases, the amplitude of this displacement component decreases, while the phase shift between the foundation motion and the free-field increases (Figure 6). The other two components of the foundation input motion (the displacement along the x-axis and the rotation about the y-axis) are the results of the cross-interaction through the soil between the two adjacent foundations; these displacement components are of equal magnitude but opposite in phase. By increasing the distance between the two foundations, the foundation input motion is reduced to the vertical displacement component, which corresponds to the motion of an isolated foundation.

For incident P-waves propagating at an angle θ in the vertical plane ($\theta = 30^\circ$ (Figure 7) and 60°), the foundation input motion presents displacement and rotation components that are now of different amplitude and different phase with respect to the free-field motion and with respect to each other. Looking at the first foundation for the case of $\theta = 30^\circ$ (Figure 7), the displacement component along the x-axis presents a slowly decreasing amplitude (of the order of 20 per cent) and an increasing phase shift with respect to the free-field motion as frequency increases. The displacement component along the vertical axis gradually becomes out-of-phase as the frequency increases while the rocking component is practically 90° out of phase with respect to the free-field motion. For the second foundation, the amplitudes of the components of the foundation motion present differences of the order of 20 per cent with respect to those relative to the first foundation, while the phase shift varies with the frequency. By increasing the distance between the two foundations, the components of the foundation input motion show a slight reduction in amplitudes for both foundations and a drastic phase shift. By increasing the angle of incidence ($\theta = 60^\circ$), the characteristics of the foundation input motion do not change although the displacements along the x-axis and the rotations about the y-axis become predominant.

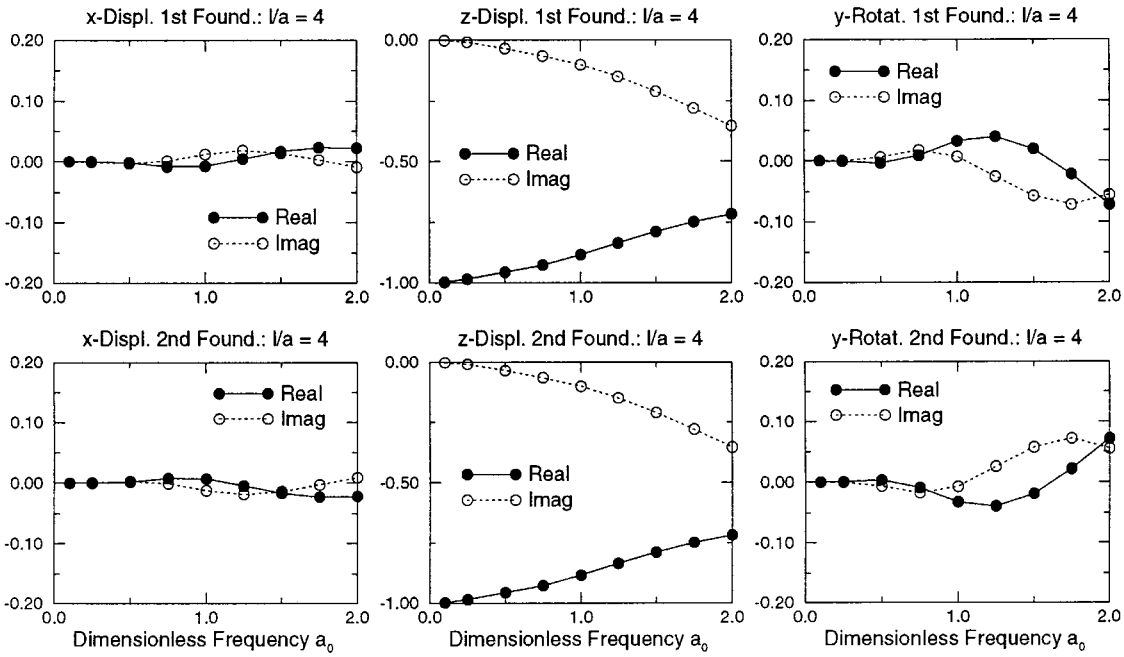

Figure 6. Foundation input motion: vertical P-waves ($\theta = 0^\circ$, $\gamma = 0^\circ$, $1/a = 4$, $h/a = 0{\cdot}5$)

© 1997 John Wiley & Sons, Ltd.

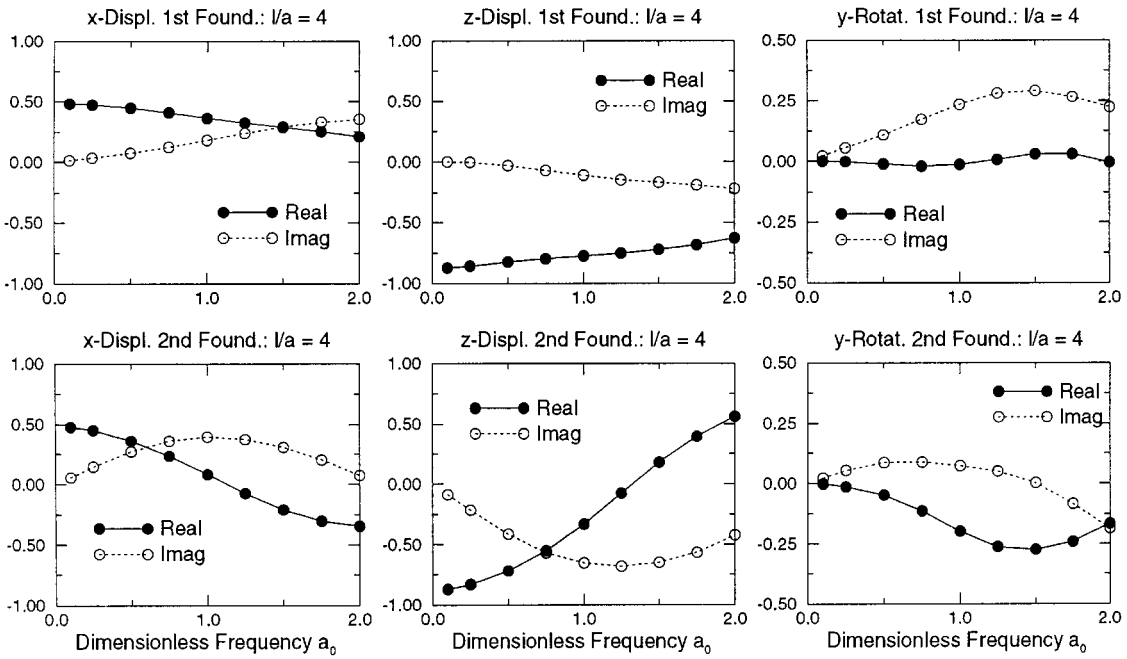

Figure 7. Foundation input motion: inclined P-waves ($\theta = 30°$, $\gamma = 0°$, $1/a = 4$, $h/a = 0{\cdot}5$)

In the case of P-waves impinging at an angle γ in the horizontal plane, each foundation presents six nonzero displacement components. For the case of $\gamma = 45°$ and $\theta = 30°$ and dimensionless distance $l/a = 4$, each of the two foundation blocks present two horizontal displacements that are almost equal in magnitude and phase. Minor differences are associated with the cross-interaction effects. Such effects are more evident in the rocking components about the x- and y-axis. For both foundations, these components are almost in phase in the low-frequency range and present an amplitude which increases with frequency. These characteristics of the foundation input motion are maintained when the distance between the two foundations increases.

Foundation input motion: incoming SV-waves

Similar conclusions can be obtained for the foundation input motion of two adjacent foundations in the case of incoming SV-waves. For vertically propagating waves, the two foundations present identical horizontal displacement and rocking about the y-axis (Figure 8). The vertical displacements are the result of the cross-interaction effects: the amplitude is very small but the phase shift between the two foundations is about 180°. In the case of inclined SV-waves ($\theta = 25°$), the motions of the two foundations present significant differences in both magnitude and phase (Figure 9). In the case of SV-waves, the angle $\theta = 25°$ has been selected such that no horizontal compressional wave, with depth decreasing amplitude, is generated. The components of the foundation input motion of the two foundations are almost identical in amplitude and slightly shifted in phase in the low-frequency range while, at high frequencies, they show significant differences (up to 80 per cent). Inclining the waves also in the horizontal plane excites all six components of the foundation input motion for each of the foundation blocks, components that varies in amplitude as well as in phase.

 © 1997 John Wiley & Sons, Ltd.

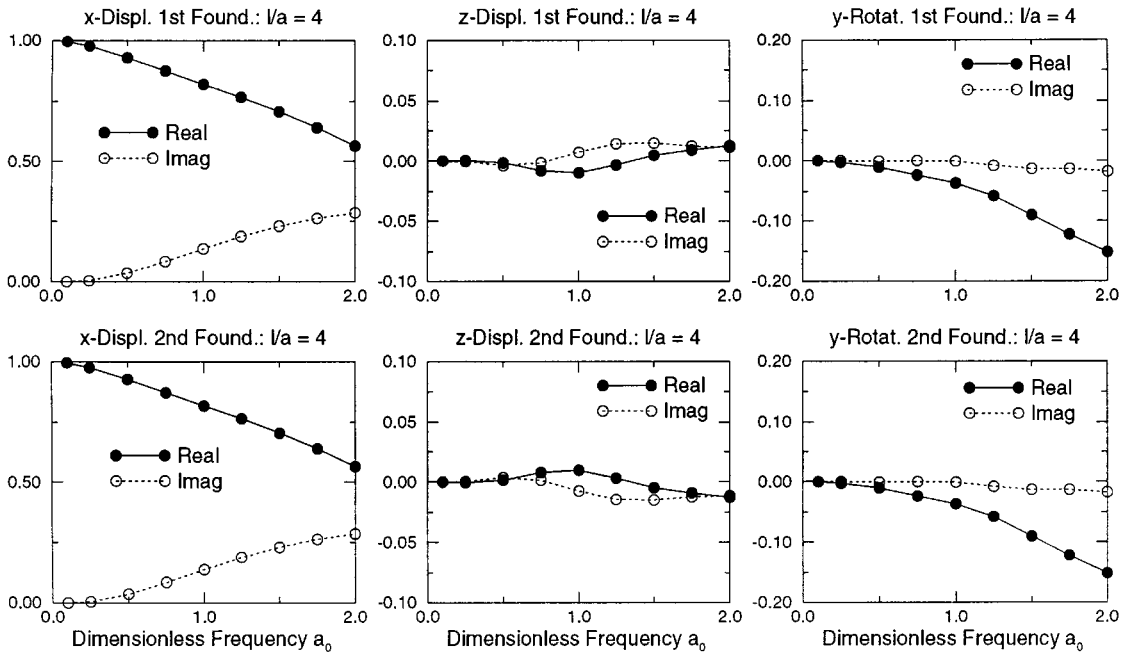

Figure 8. Foundation input motion: vertical SV-waves ($\theta = 0°$, $\gamma = 0°$, $1/a = 4$, $h/a = 0{\cdot}5$)

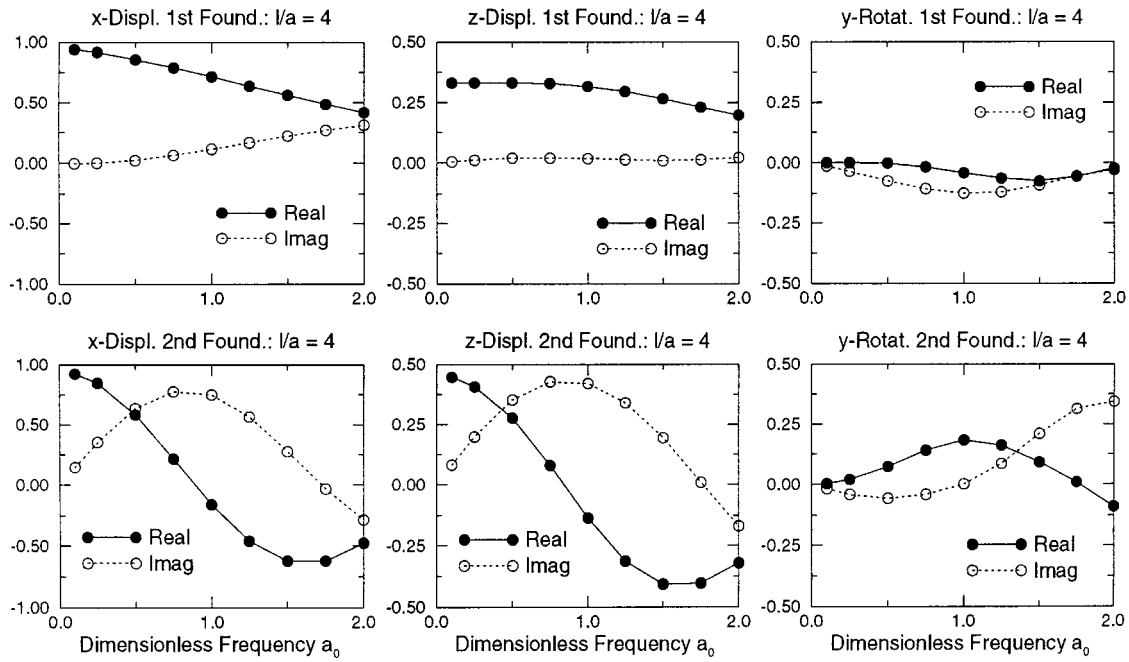

Figure 9. Foundation input motion: inclined SV-waves ($\theta = 25°$, $\gamma = 0°$, $1/a = 4$, $h/a = 0{\cdot}5$)

© 1997 John Wiley & Sons, Ltd.

CONCLUSIONS

In this study, an efficient methodology for the analysis of the cross-interaction between three-dimensional embedded foundations is presented. The approach is based on a direct boundary element formulation of the substructure deletion method and it is particularly suitable for multiple foundations of arbitrary shape. The main advantages of this proposed approach are: (1) both the exterior and the interiors problems are analysed using the boundary element method, (2) compared with a classical boundary element formulation, it does not require either the discretization of the flat surface between the foundations or the truncation of the distant free surface, and (3) it can be used for foundations of any arbitrary geometrical shape and spatial location. In the test cases analysed in this study, the cross-interaction between two rigid square foundations has been analysed for two values of the embedment ratio ($h/a = 0{\cdot}333$ and $0{\cdot}5$) and of the dimensionless distance ($l/a = 4$ and 10). Impedance functions and foundation input motion for incoming SH-, P- and SV-waves, arbitrarily inclined in both the vertical and horizontal planes, have been obtained and compared with the values corresponding to an isolated foundation. In the low-frequency range, translational, rocking and torsional components of the impedance matrix show clear effects of the cross-interaction (up to 30 per cent) which tend to disappear as the frequency and distance between the adjacent foundations increase. With regard to the foundation input motion associated with incoming SH-, P-, and SV-waves, the case of vertically propagating waves is very indicative of the cross-interaction effects. With respect to each other, the two foundations present displacement and rotational components that are either in phase or 180° out-of-phase while, with respect to the free-field, they move with a phase shift that varies with frequency. By increasing the distance between the two foundations, each component of the foundation input motion approaches the corresponding one for the case of an isolated foundation. For incoming seismic waves propagating at an angle in both the vertical and horizontal planes, the motion of the two foundations become more complicated, showing clear differences in both amplitude and phase.

ACKNOWLEDGEMENT

The author wishes to acknowledge Prof. E. de Mesquita Neto, of the FEM/UNICAMP (Brazil), and Prof. E. Romanini, of UFMS (Brazil), for their useful suggestions and discussions during the preparation of this paper. The numerical computations presented in this study were obtained using the advanced supercomputing facilities of the Cornell Theory Center, whose generous support has been greatly appreciated.

REFERENCES

1. G. B. Warburton, J. D. Richardson and J. J. Webster, 'Forced vibrations of two masses on an elastic half-space', *J. Appl. Mech. ASME* **38**, 148–156 (1971).
2. H. L. Wong and J. E. Luco, 'Dynamic interaction between rigid foundations in a layered half-space, *Soil Dyn. Earthquake Engng.* **5**, 149–153 (1986).
3. Th. Triantafyllidis and Th. Neidhart, 'Diffraction effects between foundations due to incident Rayleigh waves, *Earthquake Eng. Struct. Dyn.* **18**, 815–836 (1989).
4. Y. Wang, R. K. N. D. Rajapakse and A. H. Shah, 'Dynamic interaction between flexible strip foundations', *Earthquake Eng. Struct. Dyn.* **20**, 441–454 (1991).
5. J. Qian, L. G. Tham and Y. K. Cheung, 'Dynamic cross-interaction between flexible surface footings by combined BEM and FEM', *Earthquake Eng. Struct. Dyn.* **25**, 509–526 (1996).
6. S. D. Werner, L. C. Lee, H. L. Wong and M. D. Trifunac, 'Structural response to traveling seismic waves', *J. Struct. Div. ASCE* **105**, 2547–2564 (1979).
7. J. E. Luco and L. Contesse, 'Dynamic structure–soil–structure interaction', *Bull. Seism. Soc. Am.* **63**, 1289–1303 (1973).
8. A. M. Abdel-Ghaffar and M. D. Trifunac, 'Antiplane dynamic soil–bridge interaction for incident plane SH-waves, *Earthquake Eng. Struct. Dyn.* **5**, 107–129 (1977).
9. J. Lysmer, H. B. Seed, T. Udaka, R. N. Hwang and C. F. Tsai, 'Efficient finite element analysis of seismic soil structure interaction, *Report No. EERC* 75-34, Earth-quake Engineering Research Center, University of California, Berkeley, CA, 1975.
10. H.-T. Lin, J. M. Roesset and J. L. Tassoulas, 'Dynamic interaction between adjacent foundations', *Earthquake Eng. Struct. Dyn.* **15**, 323–343 (1987).
11. S. Wang and G. Schmid, 'Dynamic structure–soil–structure interaction by FEM and BEM', *Comput. Mech.* **9**, 347–357 (1992).

 © 1997 John Wiley & Sons, Ltd.

12. G. Dasgupta, 'Foundation impedance matrices by substructure deletion', *J. Engng. Mech. Div. ASCE* **106**, 517–524 (1980).
13. E. Mesquita Neto, E. Romanini and B. R. de Pontes, Jr., 'A boundary element implementation of the substructure deletion method', *Proc. Boundary Element*, Vol. 17, Computational Mechanics Publications, 1995, pp. 375–386.
14. R. Betti and A. G. Abdel-Ghaffar, 'Analysis of embedded foundations by substructure deletion method', *J. Engng. Mech. ASCE* **120**, 1283–1303 (1994).
15. J. E. Luco, 'On the relation between radiation and scattering problems for foundations embedded in an elastic half-space, *Soil Dyn. Earthquake Engng* **5**, 97–101 (1986).

© 1997 John Wiley & Sons, Ltd.